DFT/Electrostatic Calculations of pK_a Values in Cytochrome *c* Oxidase

Dragan M. Popović, Jason Quenneville, and Alexei A. Stuchebrukhov*

Department of Chemistry, University of California, One Shields Avenue, Davis, California 95616

Received: August 2, 2004; In Final Form: October 28, 2004

Using classical electrostatic calculations (Popovic, D. M.; Stuchebrukhov, A. A. *J. Am. Chem. Soc.* **2004**, *126*, 1858), earlier we examined the dependence of the protonation state of bovine cytochrome *c* oxidase (*CcO*) on its redox state. Based on these calculations, we have proposed a model of *CcO* proton pumping that involves His291, one of the Cu_B histidine ligands, which was found to respond to redox changes of the enzyme Fe_{a3}-Cu_B catalytic center (Popovic, D. M.; Stuchebrukhov, A. A. *FEBS Lett.* **2004**, *566*, 126). In this work, we employ combined density functional and continuum electrostatic calculations to evaluate the pK_a values of His291 and Glu242, two key residues of the model. The pK_a values are calculated for different redox states of the enzyme, and the influence of different factors on the pK_a's is analyzed in detail. The calculated pK_a values of Glu242 are between 9.4 and 12.0, depending on the redox state of the protein, which is in excellent agreement with recent experimental measurements. Assuming the reduced state of heme a_3, His291 of the oxidized Cu_B center possesses a pK_a between 2.1 and 4.0, while His291 of the reduced Cu_B center has a pK_a above 17. The obtained results support the proposal that the His291 ligand of the Cu_B center in *CcO* is a proton pump element.

I. Introduction

Cytochrome *c* oxidase (*CcO*) is the terminal enzyme of the respiratory electron transport chain in mitochondria of eukaryotes and in aerobic bacteria. It catalyzes the reduction of oxygen to water and utilizes the free energy of the reduction reaction for proton pumping across the inner-mitochondrial membrane, a process which results in a membrane electrochemical proton gradient.[3−7] The chemical reaction requires that for each O_2 molecule 4 electrons and 4 protons are delivered to the heme a_3/Cu_B catalytic center. In addition, 4 protons are pumped across the membrane.[6,7] Hence, a total of 8 charged particles are translocated across the membrane during a single turnover of the catalytic cycle of the enzyme. Electrons are transferred to the heme a_3/Cu_B catalytic site via two additional redox cofactors: Cu_A and heme *a* (see Figure 1). Both chemical and pumped protons are delivered along the *K*- and *D*-channels, of which the majority (up to 7 protons) are moving along the *D*-channel.[8,9] Although the structure of *CcO* has been solved for several organisms, the molecular mechanism of proton pumping remains largely unknown. A detailed review of the enzyme structure together with recent experimental work on the kinetics of coupled electron and proton transfer reactions in the enzyme is available in refs 3−5 and 8−12.

In our recent study,[1] continuum electrostatic calculations were employed to investigate the dependence of the protonation state of cytochrome *c* oxidase from bovine heart[13] on its redox state. On the basis of the classical electrostatic calculations, a possible mechanism of redox-linked proton pumping has been proposed. The key element of the proposed scheme is His291, one of the Cu_B ligands, which works as the proton loading site of the pump.[2] The major premise is that there is a kinetic gating of the pump.[14] Each electron delivered to the heme/copper center requires a proton to be delivered nearby, as in the "electroneutrality principle" suggested by Rich.[15] The favored kinetic pathway brings a proton from Glu242 to one of the Cu_B ligands, His291. This histidine is "above" the binuclear center and is proposed to be the key position in the exit pathway of the

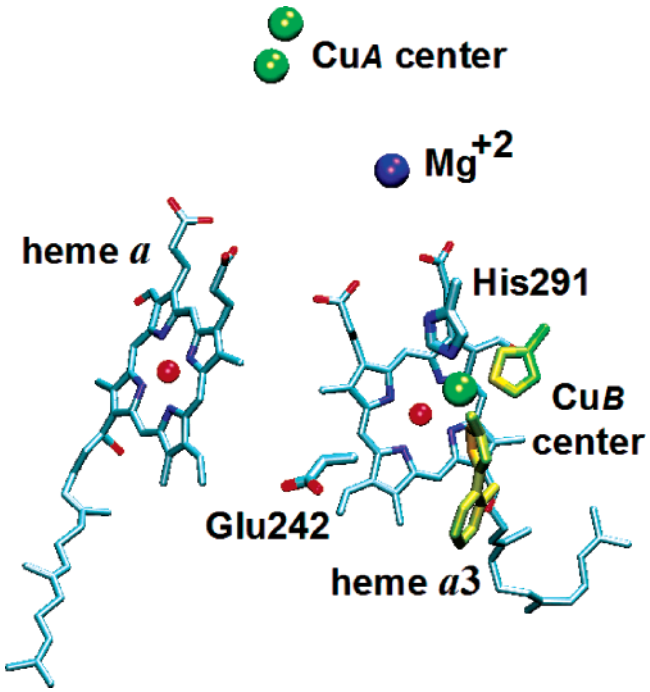

Figure 1. The relative position of the four metal redox-active centers (Cu_A, heme *a*, heme a_3, and Cu_B complex) and the two protonatable sites (Glu242 and His291 residues). According to a model proposed in ref 2, a stepwise electron transfer that brings an electron from Cu_A to the binuclear center (consists of heme a_3 and Cu_B complex) is coupled to proton translocation from Glu242 to His291 group, which serves here as a proton-loading site of the pumping mechanism in *CcO*. The position of an additional redox-inactive metal center, Mg^{2+}, is also shown.

* To whom correspondence should be addressed. Fax: 530-752-8995. E-mail: stuchebr@chem.ucdavis.edu.

10.1021/jp046535m CCC: $30.25
Published on Web 02/02/2005

pumped proton, see Figure 1. There is a rationale for this fast pathway that is based on structural considerations. Thus upon electron transfer (ET), the first proton (fast reaction) is transferred to the proton-loading site (His291), while subsequent transfer of the second "chemical" proton to the binuclear center (slow reaction) is accompanied by the ejection of the first proton.

The role of the Glu242 group in the proton translocation through *CcO*, as a proton donor of all 4 pumped and 2−3 chemical protons, is experimentally well established.[8,9,16,17] However, experimental proof for the proton pumping via the His291 as a proton-loading site is still lacking.[18] The protonation changes of this histidine are also part of the various histidine cycle models previously proposed by Wikström,[19] albeit in a very different context compared to our model. Because of the paramagnetic nature of the binuclear complex, an experimental determination of its pK_a value is not trivial. Also, the proposed His cannot be mutated without a loss of activity and therefore its theoretical role cannot be easily tested by experimental methods. On the other hand, quantum chemical methods give the possibility to computationally estimate the pK_a values to a reasonable level of accuracy and therefore present a powerful tool.[20−24] A recent study of the pK_a of histidine ligands of the iron−sulfur cluster, similar to our work, suggests that redox-dependent protonation changes of one of the histidines may be responsible for the pH-dependent redox potential of the Rieske protein.[25]

In our companion paper,[26] we used density functional theory (DFT) to calculate aqueous phase absolute pK_a values of the histidine ligand in the oxidized and reduced Cu_B complex. In addition, to roughly estimate pK_a's of His291 in *CcO*, the protein environment was mimicked as a low dielectric continuum of $\epsilon = 4$ without including the protein charges. The obtained results suggest the redox-dependent protonation state of the His291 site. However, more accurate evaluation of the pK_a's in the protein requires that the inhomogeneity of the protein dielectrics and the effects of the protein charges be taken into account, which in turn have to be found in a self-consistent manner reflecting the appropriate proton distribution for the corresponding redox state of metal centers. This is the subject of the work presented here. Moreover, for this enzyme to work as a proton pump with His291 as its proton-loading site, in addition to redox-dependence of the pK_a of His291, its pK_a should correlated with that of Glu242, an experimentally established proton donor[8,9,16,17] in *CcO* pumping (for the relative position of the two sites, see Figure 1).

In this work, we combine density functional theory and continuum electrostatics calculations to evaluate pK_a values of His291 and Glu242. The pK_a values of these residues are calculated for different redox states of the enzyme, and the effects of different structural factors of the protein on the pK_a's are analyzed in detail. The results described in this paper support the proposal[1,2] that the His291 ligand of the Cu_B center in *CcO* can work as a proton pump element.

II. Computational Methodology

The combination of the DFT and electrostatic calculations has been used successfully in the past to compute the pK_a values and redox potentials in various enzymes and proteins.[21,25,27−29] This approach takes advantages of both methods by combining the accuracy of quantum chemical calculations with a detailed description of electrostatic interactions of the whole protein. Density functional theory is applied to a relatively small quantum-mechanical (QM) system of interest to optimize its geometry, to evaluate electronic energies, and to obtain the atomic partial charges for different redox and protonation states of the complex. Electrostatic calculations, on the other hand, are used to evaluate the solvation energy of the complex in the protein environment and the Coulomb interactions of the complex with protein charges. Both the polarization of the protein medium and the protein charges affect the electron distribution of the complex; therefore the electrostatic and DFT calculations are carried out in a self-consistent way. This method was shown to produce pK_a values in proteins that are generally in good agreement with experimental data.[20−23,25]

1. Overview. A detailed review of the DFT/electrostatic method can be found elsewhere.[20,28,29] Here we only briefly summarize this approach and introduce different energy terms of the pK_a calculations, which are reported in this paper. In the discussion we divide the whole system into an active site complex (QM system) and the surrounding medium: protein, membrane, and the external aqueous phase.

The pK_a value is related to the free energy of deprotonation in aqueous solution (ΔG_{aq}^{deprot}), which is a sum of two contributions: the free energy of deprotonation in a vacuum (ΔG_{vac}^{deprot}) and the solvation energy difference between the deprotonated and protonated forms of the protonatable group (ΔG_{solv}^{deprot}),

$$pK_a = \frac{1}{kT \ln 10}(\Delta G_{aq}^{deprot}) = \frac{1}{kT \ln 10}(\Delta G_{vac}^{deprot} + \Delta G_{solv}^{deprot}) \quad (1.1)$$

These terms can be evaluated by using a thermodynamic cycle,[30,31] and the absolute value of pK_a can be determined, as explained in ref 26 (see also ref 25). Alternatively, one can compute the pK_a *shift* of the group of interest relative to a suitable model compound, and by using the experimentally determined pK_a value of the model compound, evaluate the pK_a of the group as

$$pK_a^{site} = pK_a^{model} + \Delta pK_a \quad (1.2)$$

The relative shift of the group's pK_a with respect to the model compound can be expressed as

$$\Delta pK_a = \frac{1}{kT \ln 10}\Delta\Delta G_{shift} = \frac{1}{kT \ln 10}(\Delta\Delta E_{elec} + \Delta\Delta G_{solv}) \quad (1.3)$$

where $\Delta E_{elec} = \Delta E_{elec}^{depr} - \Delta E_{elec}^{prot}$ is a quantum-mechanically calculated electronic energy difference in the gas phase between the deprotonated and protonated forms, and $\Delta\Delta E_{elec}$ is its shift relative to the model compound; $\Delta G_{solv} = \Delta G_{solv}^{depr} - \Delta G_{solv}^{prot}$ is the difference in solvation energy between the deprotonated and protonated forms, and $\Delta\Delta G_{solv}$ is the shift of the solvation energy relative to the model compound. (In eq 1.3, when the *difference* of pK_a's is computed between two compounds, the free energy of a solvated proton as well as some entropy contributions cancel out; thus, e.g., only electronic energy, i.e., the enthalpic part, of the vacuum part remains. For details, see ref 25.)

The total solvation energy (x = deprotonated or protonated form) is divided into several components:

$$G_{solv}^{x} = G_{Born}^{x} + G_{strain}^{x} + G_{q}^{x} \quad (1.4)$$

The Born solvation energy (G_{Born}^{x}) and the energy of interaction with protein charges (G_{q}^{x}), also known as the reaction and protein field terms, respectively, are two main contributions to the free energy of solvation of the active site complex in the

protein environment. The third term (G^{x}_{strain}) is the so-called "strain" energy; this term reflects the energy cost associated with the reorganization of the electronic density distribution of the active site complex induced by the reaction field of the polarized medium. (The origin of this term is as follows. The charges of the QM system polarize the surrounding medium; in turn, the induced polarization of the medium slightly changes the charge distribution of the QM system, compared with the initial charge distribution in the vacuum.)

The pK_a of the active site complex can finally be calculated as

$$pK_a^{\text{site}} = pK_a^{\text{model}} + \frac{1}{kT \ln 10}(\Delta\Delta E_{\text{elec}} + \Delta\Delta G_{\text{Born}} + \Delta\Delta G_{\text{strain}} + \Delta\Delta G_q) \quad (1.5)$$

The calculation itself is a stepwise procedure. First, we use standard DFT computation to optimize the structures of the Cu_B complex in vacuum and to obtain the electronic gas phase energies for different redox states of copper and different protonation states of His291. The same was done for the model compounds, 4-methyl-δ-imidazole and propionic acid. DFT self-consistent reaction field calculations (DFT-SCRF, see below) on the Cu_B model system embedded in a continuum dielectric of $\epsilon = 4$ or $\epsilon = 80$ were also employed to determine the strain energies and the ESP fitted atomic point charges for the active site complex. These atomic charges are in the next step used in solvation electrostatic calculations to obtain the solvation energy of the active site model in various dielectric environments.

To correctly describe the effects of the protein charges on the pK_a of His291 or Glu242, the equilibrium proton distribution in *CcO* for the corresponding redox state of metal centers is required. To this end, we performed the standard continuum electrostatic calculations (program MULTIFLEX)[32] to determine the equilibrium protonation state of the titratable residues in *CcO* for different redox states of the enzyme. In different redox states the equilibrium proton distribution is slightly different due to the proton uptake from the solution (aqueous phase) and much different from the standard protonation state.

By using the appropriate set of ESP fitted charges for the Cu_B center and the corresponding charges for the rest of the protein, we employed the solvation electrostatic calculations (MEAD program suite)[33] in a three-dielectric medium ($\epsilon_{\text{vacuum}} = \epsilon_{\text{QM system}} = 1$, $\epsilon_{\text{protein}} = 4$, and $\epsilon_{\text{solvent}} = \epsilon_{\text{aqueous phase}} = 80$) to compute the solvation of the Cu_B complex in protein. The details of the employed techniques are given in the following subsections.

2. Density Functional Calculations. The starting structure of the active site was taken from the X-ray crystal structure of bovine heart cytochrome *c* oxidase obtained by Yoshikawa et al., at 2.3 Å resolution (PBD code, 2OCC).[13] The QM model (Figure 2) used to calculate the pK_a of a Cu_B ligand consists of the Cu atom, methylimidazole molecules representing coordinated histidines 240, 290, and 291, a methyl group representing tyrosine 244 (which is cross-linked to H240), and an H_2O Cu_B-ligand. The methyl groups attached to the imidazoles represent the β-methylene groups of histidine.

Energies of each coupled protonation/redox state of the complex were calculated using DFT[34,35] and the Jaguar 5.5 quantum chemistry package.[36] All calculations used the hybrid density functional B3LYP,[37] and open shell electronic configurations (for oxidized Cu_B) were calculated with restricted open-shell DFT. Reported energies used the LACV3P+* basis set, while geometry optimizations used LACVP+*, as abbreviated

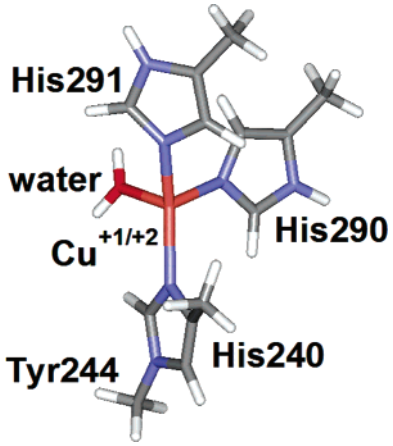

Figure 2. The model of the Cu_B center used in the pK_a calculation of His291.

in the Jaguar program.[36,38] These basis sets include nonrelativistic electron core potential for the Cu atom. The basis sets for the metal valence electrons (and all nonmetal electrons) are of split valence quality (6-31+G*)[39−44] for LACVP+* and triple split valence quality (6-311+G*)[45−48] for LACV3P+*. They include polarization and diffuse functions for all heavy atoms.

Geometry optimizations were conducted in Cartesian space, in vacuum. In the procedure, the Cu atom, the ligating ϵ-nitrogen and methyl group of methylimidazoles were kept fixed. This scheme allows relaxation of the remaining atoms while preserving the integrity of the crystal stucture with respect to both the unique Cu-ligand geometry as well as the attachment location of the histidines to the protein backbone. Four optimizations were performed: for the protonated and deprotonated forms of His291, and each of these for oxidized and reduced Cu_B. The geometry of the Cu-ligated water molecule was set using molecular mechanics. This water molecule is known to be very weakly bound and quite mobile.[49,50]

To quantify the effect of the electronic reorganization of the solute and to obtain the corresponding set of the ESP fitted charges for the QM considered system, the complex was surrounded by a continuum dielectric ($\epsilon = 4$ or 80) and the SCRF method was applied as implemented in Jaguar 5.5.[51,52] The probe radius of the surrounding dielectric was set to 1.4 Å, and the standard Jaguar set of the van der Waals radii for atoms was used. The ESP atomic charges were generated by using a modified version of the CHELPG procedure of Breneman and Wiberg.[53]

3. Classical Electrostatic Calculations. The protonation states of the titratable residues in *CcO* for different redox states of the enzyme were determined as described in ref 1. The Poisson−Boltzmann equation was solved numerically[54−63] for the inhomogeneous dielectric of the protein−membrane−water system with the program MEAD.[33] The protonation state sampling was subsequently done by employing a Monte Carlo titration technique as implemented in program KARLSBERG.[64] The electrostatic calculations were performed on chains A and B, which belong to monomer I from the crystal structure of mitochondrial *CcO* from bovine heart (PDB code, 2OCC).[13] In our calculations, the membrane is modeled as a low dielectric slab of 45 Å that covers the central part of the enzyme. Taking a thermodynamic average over different protonation states of the titratable groups, one can evaluate the equilibrium charge distribution in *CcO* for the given temperature, pH, and redox state of metal centers. The obtained charge distribution of the protein is used in electrostatic calculations of the solvation

energy term G_q^x, eq 1.4. We found that using the standard protonation state of the protein leads to completely erroneous results.

4. Solvation Calculations. Once the charges of the active site complex have been calculated, its geometry has been optimized, and an equilibrium charge distribution of the protein has been obtained, the DFT optimized active site cluster needs to be inserted back into the protein in order to set up the electrostatic solvation calculations. The MEAD program[33] has been used to calculate the solvation energy of the quantum-chemically treated cluster in the aqueous phase, in a continuum low dielectric medium, or in the protein (see below all different models). Solvation of the active site cluster in the protein consists of two main contributions: the Born solvation energy and the energy of the interaction with the protein charges (reaction and protein field energies).

The Poisson equation (or Poisson−Boltzmann equation (PBE)) is solved numerically for the system divided into three dielectric regions represented by dielectric constants of 1, 4, and 80, for the quantum-chemically considered active site, a protein, and the solvent region, respectively. Such choice of the values for the dielectric regions is physically reasonable and very well supported by numerous studies.[65−68] Using $\epsilon_{\text{protein}} = 4$ approximately compensates the effects of electronic and nuclear polarization allowing some mobility of the protein dipoles and reorientational relaxation of the protein,[28] which otherwise are not explicitly taken into account. However, in the QM considered system, electronic and nuclear degrees of freedom are treated explicitly, no additional shielding is required, and therefore $\epsilon_{\text{QM system}} = 1$. $\epsilon_{\text{water}} = 80$ is traditionally used in continuum solvent electrostatic calculations to describe the screening properties of the aqueous phase.

In these calculations, the ESP fitted charges are used for the QM system, while partial charges of the protein atoms are taken from the CHARMM22 parameter set,[69] modified so as to reflect the equilibrium protonation state of the enzyme. The backbone atoms of the Cu_B ligands are also included in electrostatic calculations. They affect the energetics through the influence of the background charges (so they are not part of the QM system). The protein charges and radii that we use in this application have been used successfully before to calculate the electrostatic energies, protonation probabilities of titratable groups, and redox potentials of cofactors in different proteins.[1,62,63]

The electrostatic potential for the system was solved by the Poisson equation (PE) with a three-step grid focusing procedure. The lattices with highest resolution were centered at the active site cluster. The probe radius of the surrounding dielectric was set to 1.4 Å. Ionic strength was set to 0, since we found earlier that the mobile ions do not make any significant contribution to the calculated potentials in the interior of the *CcO*, where the active site complex is located.[1]

The pK_a's of His291 and Glu242 reported here were calculated using the equilibrium protonation states of the enzyme, which were determined as in our previous work[1] for each redox state involved. The pK_a's of all groups in the enzyme should be calculated in a self-consistent manner, and in general, the protonation state of the rest of the protein should depend on the protonation state of the selected group. Here the self-consistency is easily achieved, because the found protonation state of His291 and Glu242 is either essentially 1 or 0, depending on the redox state of the enzyme.

To examine the strength of the coupling of the protonation state of His291 and other protonatable groups of the protein, two sets of charges for the protein were obtained: for protonated and for deprotonated states of His291. The pK_a values of His291 determined for these two sets of charges were found to differ by less than 0.3 pK_a units.

III. Results and Discussion

1. Computational Models. To get a sense of how different factors affect the apparent pK_a values of His291 and Glu242, we considered several computational models shown in Figure 3.

Model a represents the quantum-chemically (QM) treated system, Figure 2, solvated in a continuum dielectric of $\epsilon = 80$. Using this model, we obtain the pK_a values of the groups in water.

Model b is the same as model a, only for dielectric $\epsilon = 4$. The pK_a's obtained from this model should illustrate the magnitude of the effect of the low dielectric environment of the protein.

Model c adds protein charges to the uniform dielectric of $\epsilon = 4$. This is still a very rough description of the protein system because the complexity of the protein−solvent surface, inner water-filled cavities, and solvent itself is missing.

Model d introduces the inhomogeneity of the dielectric medium represented by the inner water cavities with $\epsilon = 80$, shape of the protein, membrane, and the outside aqueous phase. No protein charges are present here.

Finally, model e includes all components of the protein system: inhomogeneity of the dielectic environment, as in model d, and protein charges, as in model c.

2. The Calculation of pK_a in Water. As explained in the methods section, to calculate pK_a's in a protein, we first calculate the pK_a values of the corresponding groups in water. For a calculation of the pK_a values of the δ-nitrogen of the His291 ligand of the Cu_B complex, we use methylimidazole (MeIm) as a reference compound, for which the experimental pK_a is known. The experimental value of pK_a of the δ-nitrogen of MeIm is 6.6. Using this value and the difference in electronic and solvation energies between MeIm and the Cu_B model complex, we can evaluate the pK_a value of the latter in the aqueous phase. The results are presented in Tables 1 and 2. (Here and later in the text, by protonated and deprotonated forms of MeIm we mean protonated and deprotonated δ-nitrogen of the compound, i.e., cationic and neutral forms of MeIm. Similarly, protonated and deprotonated forms of the Cu_B center mean protonated and deprotonated δ-nitrogen of the His291 ligand.)

Table 1 lists the calculated values of the solvation energy changes of MeIm and the Cu_B complex upon protonation of these compounds. There are two contributions: the electronic reorganization energy contribution (due to solvent back reaction), which is called the "strain" energy, and the Born solvation energy. The total solvation energy is the sum of these two contributions.

Table 2 lists the calculated pK_a values of His291 of the Cu_B complex together with individual contributions of electronic and solvation energy and the corresponding data for the reference compound MeIm. Here, the electronic energy difference in the gas phase between the deprotonated and protonated forms (ΔE_{elec}), a shift of the electronic gas phase energy relative to the MeIm model compound ($\Delta\Delta E_{\text{elec}}$), the difference in aqueous phase solvation energy between the two forms (ΔG_{solv}), a shift of the solvation energy relative to the model compound ($\Delta\Delta G_{\text{solv}}$), and the total shift in kcal/mol and pK_a units are given separately to show their individual contributions to pK_a values.

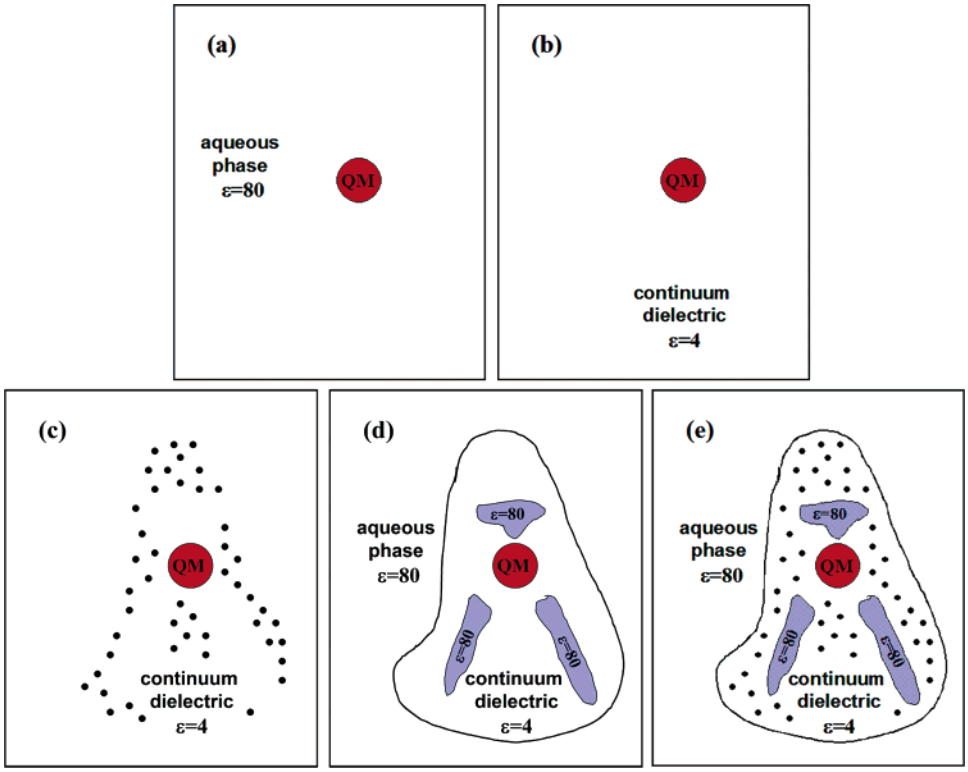

Figure 3. Schematics of different models used in this study. In model a, the QM system that consists of the Cu_B center and coordinated ligands (with dielectric constant $\epsilon = 1$ inside) is solvated in the aqueous phase. (b) The QM system is solvated in a low dielectric of $\epsilon = 4$. (c) The QM system is embedded in a continuum dielectric of $\epsilon = 4$ and surrounded with protein charges. (d) The QM system is embedded in an inhomogeneous dielectric medium represented by $\epsilon = 4$ within the borders of the protein and $\epsilon = 80$ inside the inner water-filled cavities and outside of the protein, while protein charges are neglected. Model e includes a full protein−solvent description including dielectric inhomogeneities and protein charges, whereas the QM system is treated by the DFT method. Crystallographically, more than 150 water molecules have been found in the inner protein cavities (refs 80−82). Only the most important water-filled cavities are schematically shown in the figure. They represent the proton input *D*- and *K*-channels leading to the active site and the large water-filled cavity on the proton output side of the protein.

TABLE 1: Solvation Energy Difference (ΔG_{solv}, in kcal/mol) between the Deprotonated and Protonated Forms of 4-Methylimidazole and of the Cu_B Complex (Oxidized or Reduced) in Aqueous Solution[a]

compound	$E_{reorganization}$ deprotonated form	$E_{reorganization}$ protonated form	"strain" energy	Born energy	ΔG_{solv} in water ($\epsilon = 80$)
methyl-δ-imidazole	+4.0	+1.5	+2.5	+52.2	+54.7
$Cu_B^{2+}(H_2O)$ oxidized	+10.1	+3.4	+6.7	+86.7	+93.4
$Cu_B^{+}(H_2O)$ reduced	+9.5	+3.3	+6.2	+8.5	+14.7

[a] Here and elsewhere, the protonated and deprotonated forms are the corresponding states of δ-nitrogen of MeIm and the His291 ligand of the Cu_B compound (e.g., a protonated form of MeIm is a cation, while the deprotonated MeIm is a neutral form where the δ-proton gets deprotonated). The "strain" and the Born contributions are given as a difference in energy between the deprotonated and protonated forms.

TABLE 2: Calculated pK_a Values of the His291 Site in the Oxidized and Reduced Cu_B Complex in the Aqueous Phase Relative to the pK_a of the Model Compound (Methylimidazole)[a]

compound	ΔE_{elec}	$\Delta\Delta E_{elec}$	ΔG_{solv}	$\Delta\Delta G_{solv}$	$\Delta\Delta G_{shift}$	ΔpK_a	pK_a
methyl-δ-imidazole	+234.6	0	+54.7	0	0	0.0	6.6[b]
$Cu_B^{2+}(H_2O)$ oxidized	+198.7	−35.9	+93.4	+38.7	+2.8	+2.0	8.6[c]
$Cu_B^{+}(H_2O)$ reduced	+283.7	+49.1	+14.7	−40.0	+9.1	+6.6	13.2[c]

[a] The corresponding electronic and solvation contributions to pK_a calculations and their differences relative to the reference compound are also shown in the table. Energies are reported in kcal/mol. [b] Experimental value. [c] Calculated value.

The side chain of an isolated histidine has two macroscopic pK_a values of 7.0 and 14.0, for the first and the second deprotonation. Compared with methylimidazole, for which microscopic pK_a in water has been measured to be 6.6 (for the Nδ-site proton),[70] the equivalent histidine ligated to the Cu_B metal center possesses pK_a's of 8.6 in oxidized and 13.2 in reduced form, based on our present electrostatic calculations.

3. The pK_a of His291 in *CcO*. Table 3 presents the summarized results of the electrostatic solvation calculations for the different dielectric models (models a, b, and d) applied in our study. The solvation energy of the Cu_B complex is calculated in a continuum low dielectric medium of $\epsilon = 4$ (shown in standard letters), in an inhomogeneous dielectric of protein with the dielectric boundaries which reflects the real shape of the protein (shown in bold), and in a continuum solvent of $\epsilon = 80$ (aqueous phase, shown in italics). Here we consider only the effects of the dielectric medium on solvation energies, while the effects of the surrounding protein charges are not included yet.

The solvation in an inhomogeneous dielectric of the protein region is somewhat larger than in a uniform dielectric of $\epsilon = 4$ but much smaller than in the aqueous phase. Also the "strain" energy in the aqueous phase is larger than in a low dielectric medium because the high dielectric medium polarizes the charges of the QM system much stronger than the low dielectrics can. Since the reorganization of the charge densities due to the induced polarization from the medium produces an energetic

TABLE 3: Comparison of the Solvation Energy (kcal/mol) of the Cu_B Complex in the Oxidized or Reduced State with His291 Either in Deprotonated or Protonated Form, between Continuous Aqueous Phase ($\epsilon = 80$), Uniform Low Dielectic Medium ($\epsilon = 4$), and Inhomogeneous Dielectric of Protein (Represented by $\epsilon = 4$ Inside the Protein and $\epsilon = 80$ in Water-Filled Cavities)[a]

protonation form	Born energy	"strain" energy	solvation energy	compound/dielectric medium
His291 deprotonated	−55.0	+3.4	−51.6	
	−63.4	**+3.4**	**−60.0**	$Cu_B^{2+}(H_2O)$ oxidized
	−78.3	*+10.1*	*−68.2*	
His291 protonated	−121.1	+1.5	−119.6	
	−137.9	**+1.5**	**−136.4**	
	−165.0	*+3.4*	*−161.6*	
Cu_B^{2+} oxidized, depr − prot	+66.1	+1.9	+68.0	continuum ($\epsilon = 4$)
	+74.5	**+1.9**	**+76.4**	**inhomogeneity ($\epsilon_1 = 4$, $\epsilon_2 = 80$)**
	+86.7	*+6.7*	*+93.4*	*aqueous phase ($\epsilon = 80$)*
His291 deprotonated	−33.3	+3.6	−29.7	
	−40.3	**+3.6**	**−36.7**	$Cu_B^{+}(H_2O)$ reduced
	−50.7	*+9.5*	*−41.2*	
His291 protonated	−41.1	+1.4	−39.7	
	−49.0	**+1.4**	**−47.6**	
	−59.2	*+3.3*	*−55.9*	
Cu_B^{+} reduced, depr − prot	+7.8	+2.2	+10.0	continuum ($\epsilon = 4$)
	+8.7	**+2.2**	**+10.9**	**inhomogeneity ($\epsilon_1 = 4$, $\epsilon_2 = 80$)**
	+8.5	*+6.2*	*+14.7*	*aqueous phase ($\epsilon = 80$)*
deprotonated	−12.2	+4.0	−8.2	methyl-δ-imidazole
protonated	−64.4	+1.5	−62.9	
depr − prot	+52.2	+2.5	+54.7	aqueous phase ($\epsilon = 80$)

[a] Only the effect of the dielectric medium on solvation is considered, while the effect of the surrounding protein charges is neglected. For further comparison, the solvation energy contributions from deprotonated and protonated methylimidazole in aqueous solution are also given.

TABLE 4: Total Solvation (kcal/mol) of the Cu_B Complex in a Low Dielectric Continuum of $\epsilon = 4$ and in the Protein Including the Protein Charges[a]

compound	Born energy	interaction with protein charges	"strain" energy	total solvation	redox state [A−a-a_3−B][b]/ dielectric medium
$Cu_B^{2+}(H_2O)$ oxidized, His291 deprotonated	*−55.0*	*−1.4*	*+3.4*	*−53.0*	
	−63.4	+18.6	+3.4	−41.4	
$Cu_B^{2+}(H_2O)$ oxidized, His291 protonated	*−121.1*	*−35.5*	*+1.5*	*−155.1*	OORO
	−137.9	+10.6	+1.5	−125.8	
Cu_B^{2+} oxidized, depr − prot	*+66.1*	*+34.1*	*+1.9*	*+102.1*	*continuum $\epsilon = 4$*
	+74.5	+8.0	+1.9	+84.4	protein
$Cu_B^{+}(H_2O)$ reduced, His291 deprotonated	*−33.3*	*+27.4*	*+3.6*	*−2.3*	
	−40.3	+24.7	+3.6	−12.0	
$Cu_B^{+}(H_2O)$ reduced, His291 protonated	*−41.1*	*−8.4*	*+1.4*	*−48.1*	OORR
	−49.0	+15.1	+1.4	−32.5	
Cu_B^{+} reduced, depr − prot	*+7.8*	*+35.8*	*+2.2*	*+45.8*	*continuum $\epsilon = 4$*
	+8.7	+9.6	+2.2	+20.5	protein

[a] The total solvation consists of three contributions: the Born solvation energy, the interaction with protein charges (the so-called reaction and protein field), and "strain" energy. The protonation state of the rest of the protein is the equilibrium protonation state for the corresponding redox state of the enzyme (only OORO or OORR states are shown in the table; for other redox states, see Table S1 in the Supporting Information). [b] Redox state [A−a-a_3−B] refers to the state of four redox-active metal centers: Cu_A, heme *a*, heme a_3 and Cu_B complex, respectively.

cost on the electronic gas phase energies, the strain contributions always have a positive sign.

Table 4 gives results of electrostatic calculations for models c and e. The solvation energies are compared in a uniform low dielectric of $\epsilon = 4$ and in the "real" protein. The surrounding protein charges are included here also. It is interesting to examine the differences in the reaction and protein field energies between the two models.

As expected, considering the Born energy, all four species are better solvated in an inhomogeneous protein dielectric, which includes high-ϵ water cavities, than in a continuum dielectric of low ϵ. Also, the protonated forms of each redox pair are better solvated than deprotonated ones. This is especially true for an inhomogeneous protein environment, where for instance comparing their Born energies the oxidized-protonated Cu_B complex (total charge +2) is much better solvated in the dielectric environment of *CcO* than the oxidized-deprotonated form (total charge +1). One may also expect that the Born energy of the oxidized-protonated Cu_B complex (total charge +2) should be the largest, the one of the reduced-deprotonated form (total charge 0) should be the smallest, and the oxidized-deprotonated and reduced-protonated forms (with total charges of +1) should have similar values. All discrepancies from this are due to the specific charge distributions in different species.

The effect of the interaction with the protein charges is much smaller in the "real" protein than in a uniform ϵ of 4. A continuum low dielectric medium significantly destabilizes the deprotonated form of His291 in both redox states. In the "real" protein there is a large bulb filled with water molecules around the position of the His291 site, which significantly screens the influence of the surrounding charges, and therefore the deprotonated form is less destabilized by the interaction with protein charges (∼ +35 vs +9 kcal/mol). This destabilization is mostly due to the adjacent negatively charged propionates of heme a_3 and since in both redox states, OORO and OORR, they are deprotonated, the effect of the protein charges, within the same model, gets very similar (+34.1 vs +35.8 or +8.0 vs +9.6).

Table 5 is an overview showing the difference in electronic gas phase energies and the difference in solvation energies between protonated/deprotonated forms and calculated pK_a

TABLE 5: pK_a Values of the His291 Residue as a Part of the Oxidized or Reduced Cu_B Center in Cytochrome *c* Oxidase[a]

redox state	ΔE_{elec}	$\Delta\Delta E_{elec}$	ΔG_{solv}	$\Delta\Delta G_{solv}$	$\Delta\Delta G_{shift}$	ΔpK_a	pK_a
In Aqueous Phase							
methyl-δ-imidazole	+234.6	0	+54.7	0	0	0.0	6.6
$Cu_B^{2+}(H_2O)$ oxidized	+198.7	−35.9	+93.4	+38.7	+2.8	+2.0	8.6
$Cu_B^{+}(H_2O)$ reduced	+283.7	+49.1	+14.7	−40.0	+9.1	+6.6	13.2
In Continuum Dielectric of $\epsilon = 4$ (No Protein Charges)							
$Cu_B^{2+}(H_2O)$ oxidized	+198.7	−35.9	+68.0	+13.3	−22.6	−16.5	−9.9
$Cu_B^{+}(H_2O)$ reduced	+283.7	+49.1	+10.0	−44.7	+4.4	+3.2	9.8
In Inhomogeneous Dielectric of Protein, $\epsilon = 4$ and 80 (No Protein Charges)							
$Cu_B^{2+}(H_2O)$ oxidized	+198.7	−35.9	+76.4	+21.7	−14.2	−10.3	−3.7
$Cu_B^{+}(H_2O)$ reduced	+283.7	+49.1	+10.9	−43.8	+5.3	+3.8	10.4
In Continuum $\epsilon = 4$ (Including Protein Charges)							
OORO	+198.7	−35.9	+102.1	+47.4	+11.5	+8.4	15.0
OORR	+283.7	+49.1	+45.8	−8.9	+40.2	+29.3	35.9
In Protein (Including Dielectric Inhomogeneity and Protein Charges)							
OORO	+198.7	−35.9	+84.4	+29.7	−6.2	−4.5	2.1
RORO	+198.7	−35.9	+85.7	+31.0	−4.9	−3.5	3.1
ORRO	+198.7	−35.9	+86.8	+32.1	−3.8	−2.7	3.9
RRRO	+198.7	−35.9	+87.0	+32.3	−3.6	−2.6	4.0
OORR	+283.7	+49.1	+20.5	−34.2	+14.9	+10.8	17.4
RORR	+283.7	+49.1	+21.8	−32.9	+16.2	+11.8	18.4
ORRR	+283.7	+49.1	+22.7	−32.0	+17.1	+12.5	19.1
RRRR	+283.7	+49.1	+23.6	−31.1	+18.0	+13.1	19.7

[a] The pK_a of His291 is calculated relative to the pK_a of the model compound, methylimidazole in the aqueous phase. It is shown how different dielectric medium and interaction with protein charges affect the calculated pK_a of the His291 site. Energies are reported in kcal/mol.

values for the oxidized and reduced Cu_B complex obtained in different computational models applied in our study.

The calculated aqueous phase pK_a values of the His291 ligand of the Cu_B center are 8.6 and 13.2; therefore in aqueous phase at pH 7 this complex would be protonated in both redox states. Already in a low continuum dielectric without protein charges, the pK_a value of the His site becomes redox-dependent. The His-ligand would be distinctly deprotonated with pK_a = −9.9 in oxidized and distinctly protonated in reduced state (pK_a = +9.8). Introducing the dielectric inhomogeneities but without the protein charges, the pK_a value of the oxidized Cu_B complex arises by about 6 pK_a units; however, the δ-His position remarkably is still deprotonated since its pK_a is equal to −3.7. There is not much change here in the pK_a of the reduced complex, such that the pK_a redox-dependence remains.

For a full description of the protein−solvent system, the equilibrium protein charge distribution for the given redox state of all four metal centers is also required. Assuming the reduced state of heme a_3, the pK_a of the His291 site in the oxidized Cu_B center of bovine *CcO* is between 2.1 and 4.0 depending on the redox state of other metal centers. When the binuclear center is in the two-electron reduced state, the His291 site has a pK_a above 17. In the fully reduced enzyme (FR = R_4) His291 possesses the highest pK_a of 19.7, while in the mixed-valence enzyme (MV = R_2) the pK_a of His291 is just slightly lower, i.e., 17.4. Thus, the addition of the protein charges to dielectric inhomogeneities further increases the apparent pK_a values of the His291 ligand by an additional 5.8−7.7 pK_a units for the oxidized Cu_B center and about 7−9.3 pK_a units in the corresponding reduced states of the enzyme.

TABLE 6: pK_a Values of Glu242 Residue[a]

redox state	ΔE_{elec}	$\Delta\Delta E_{elec}$	ΔG_{solv}	$\Delta\Delta G_{solv}$	$\Delta\Delta G_{shift}$	ΔpK_a	pK_a
In Aqueous Phase							
propionic acid	+357.0	0	−60.0	0	0	0.0	4.4
In Continuum Dielectric of $\epsilon = 4$ (No Protein Charges)							
Glu242	+357.0	0	−46.1	+13.9	+13.9	+10.1	14.5
In Inhomogeneous Dielectric of Protein, $\epsilon = 4$ and 80 (No Protein Charges)							
Glu242	+357.0	0	−49.5	+10.5	+10.5	+7.6	12.0
In Continuum $\epsilon = 4$ (Including Protein Charges)							
Glu242 in OORO	+357.0	0	−33.0	+27.0	+27.0	+19.6	24.0
Glu242 in OORR	+357.0	0	−32.9	+27.1	+27.1	+19.7	24.1
In Protein (Including Dielectric Inhomogeneity and Protein Charges)							
Glu242 in ORRO	+357.0	0	−49.9	+10.1	+10.1	+7.4	11.8
Glu242 in OORR	+357.0	0	−53.0	+7.0	+7.0	+5.1	9.5
Glu242 in OORO	+357.0	0	−53.1	+6.9	+6.9	+5.0	9.4
Glu242 in RRRO	+357.0	0	−50.1	+9.9	+9.9	+7.2	11.6
Glu242 in ORRR	+357.0	0	−49.9	+10.1	+10.1	+7.4	11.8
Glu242 in RRRR	+357.0	0	−49.5	+10.5	+10.5	+7.6	12.0
Glu242 in RORR	+357.0	0	−52.4	+7.6	+7.6	+5.5	9.9
Glu242 in RORO	+357.0	0	−52.4	+7.6	+7.6	+5.5	10.0
Glu242 in OOOR	+357.0	0	−53.0	+7.0	+7.0	+5.1	9.5

[a] The pK_a of Glu242 is calculated relative to the pK_a of the model compound, propionic acid in the aqueous phase. It is shown how different dielectric medium and interaction with protein charges affect the calculated pK_a of the Glu242 site. Energies are reported in kcal/mol. The electronic energy difference was obtained with the B3LYP Functional and the 6-311G** basis set which gives better agreement with experimentally measured proton affinities.

By using model c, which is the Cu_B complex embedded in a uniform low dielectric region that also includes the appropriate protein charges, the pK_a of the His291 site becomes much larger, 15 and 36 for the OORO and OORR redox state, respectively. Thus, adding the protein charges to the continuum low dielectric environment will produce a huge increase of the apparent pK_a values, by about 25 pK_a units. Compared to the more sophisticated model e, one can conclude that the difference is made by having the inhomogeneous system with the well-defined dielectric boundaries, which accounts for the shape of the protein molecule, including external solvent and introducing the water-filled cavities inside a protein where they are in reality located. It came out that the cavities inside the cytochrome *c* oxidase appear to play a very important role. Although the effect of the cavities is not so large for the Born solvation energies, the crucial role of the water-filled cavities appears to be in the screening effect on the protein charges, which can significantly change the energetics of the protonation reactions in the protein.

4. The pK_a of Glu242 in *CcO*. Table 6 summarizes the results of the pK_a calculations on the Glu242 residue for different computational models. The experimentally measured acidity of the propionic acid and a suitable model compound such as the *N*-formyl-*N*-methylamide derivative of glutamic acid in aqueous solution is 4.4.[71−73]

Our calculations show that in a low uniform dielectric of ϵ = 4, glutamate, with pK_a = 14.5, would like to be protonated. Introducing the dielectric inhomogeneities as they are in *CcO*, the pK_a value drops to 12.0. Addition of the equilibrium charge distribution for the rest of the protein for the given redox state

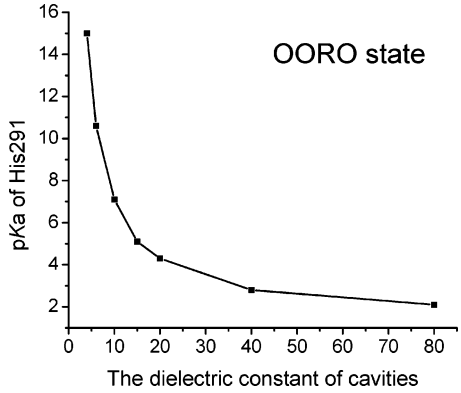

Figure 4. The pK_a dependence of the His291 residue on the dielectric constant of water-filled cavities in the OORO redox state. The obtained dependence is affected by the changes of ΔG_{Born} and ΔG_q energy terms. In addition to the expected decrease of the ΔG_q term with an increase of ϵ_{cavity}, also the Born energies of deprotonated and protonated species change in such a way that an increase of ϵ_{cavity} causes larger stabilization of the protonated form (+2) compared with the deprotonated form (+1).

of enzyme only slightly modifies the pK_a of the Glu242 residue. Depending on the redox state of the enzyme, the calculated pK_a values of Glu242 are between 9.4 and 12.0. This is in excellent agreement with recent experimental measurements. The FTIR measurements and the measurements of the pH-dependent proton transfer (PT) rates suggest that Glu242 is protonated at pH 7 with the apparent p$K_a \geq 9$.[74−79]

Based on the calculations, the pK_a value of Glu242 primarily depends on the redox state of heme *a*, and it is about 10 in redox states of the enzyme wherein heme *a* is in its oxidized state, while for the reduced heme *a*, its pK_a value is around 12. Additional study will address the question of how the pK_a of Glu242 depends on the conformation of its side chain and a mutual dependence of the protonation state of Glu242 and His291 on their pK_a's.

The effects of different factors on the pK_a values of both His291 and Glu242 are summarized in Figure 5.

5. The Dielectric Constant of Protein Cavities. In the described calculations, the cavities of the interior of the protein were assumed to be filled with water and were assigned a dielectric value of 80, as was done e.g. in refs 23, 25, 28, and 29. Indeed a lot of internal water is observed in the crystal structure of *CcO*.[80−82] There is a significant degree of ambiguity, however, in the dielectric constant of these water-filled cavities. A discussion of the appropriate value of the dielectric of the cavities is beyond the scope of this paper; we therefore explore here only the dependence of the main results and qualitative conclusions on the possible values of this important parameter of the model.

To clarify the importance of water-filled channels and cavities, we examine how the pK_a's of Glu242 and His291 depend on the dielectric constant associated with the protein cavities. Figure 4 shows a dependence of the His291 pK_a on the dielectric constant of cavities. Here, the dependence is shown only for the OORO redox state of the enzyme, which is the most critical for the whole model of proton pumping via His291 as the proton-loading site. More detailed information on this dependence is presented in Table 7, where results are shown for the various ϵ values of the cavities.

There is experimental evidence that water molecules inside *CcO* are quite mobile.[83−85] First of all, the enzyme produces the water molecules in the binuclear center and on a time scale of 10 ms they leave the active site and their appearance is noted near the position of the Mg-center (in electron paramagnetic resonance measurements using isotopic $^{17}O_2$).[86] Thus, the Cu_B center is located at the beginning of the so-called water exit channel(s). Second, it is believed that water molecules actively participate and facilitate a proton transfer through the enzyme,[87−89] which is associated with the significant reorganization and reorientation of water molecule dipoles. Such large mobility of

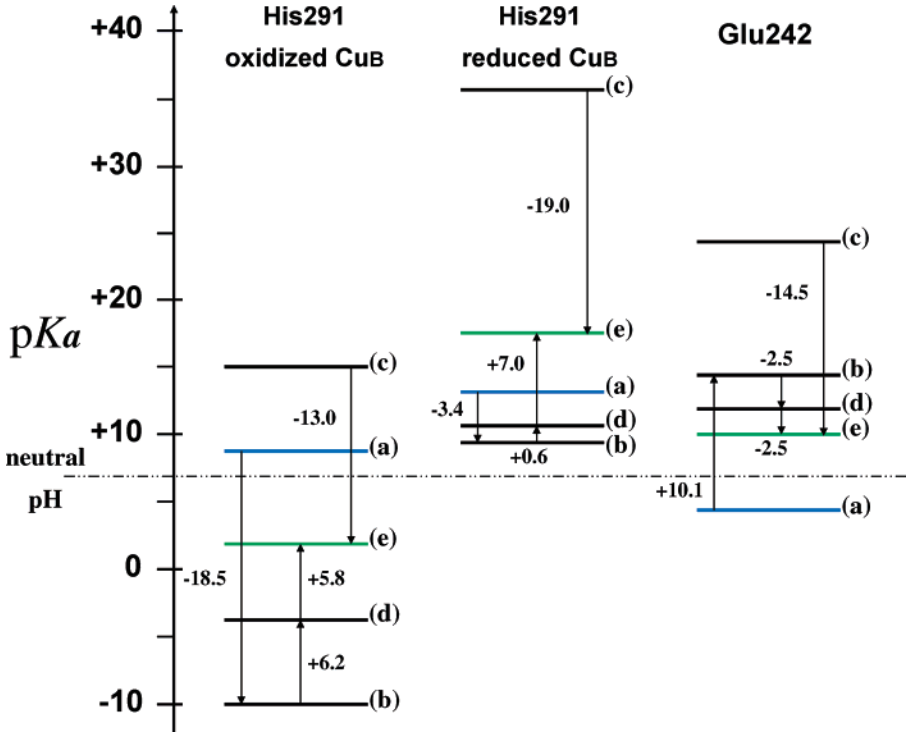

Figure 5. A schematic of the pK_a values of His291 in the oxidized and reduced Cu_B complex and the pK_a's of Glu242, for different models (models a−e) applied in our study. Blue bars are related to the pK_a values in the aqueous phase, and green bars represent the calculated pK_a's in the protein (cytochrome oxidase). The arrows with the numbers represent the magnitude of the pK_a shifts caused by the different structural effects. See the text for the explanation.

TABLE 7: pK_a's of Glu242 and His291 Site in the Different Redox States of Cytochrome *c* Oxidase[a]

	Glu242 ϵ_{cavity}			His291 ϵ_{cavity}		
redox state	15	20	80	15	20	80
OORR	12.9	11.9	9.5	22.6	21.1	17.4
OORO	13.0	12.0	9.4	5.1	4.3	2.1
RORO	13.8	12.6	10.0	6.5	5.4	3.1
ORRO	15.9	14.7	11.8	7.4	6.3	3.9
RRRO	15.8	14.6	11.6	7.7	6.5	4.0
RORR	13.7	12.6	9.9	23.8	22.3	18.4
ORRR	15.9	14.7	11.8	24.6	23.1	19.1
RRRR	16.3	15.1	12.0	25.5	23.9	19.7

[a] R stands for the reduced and O for the oxidized states of redox cofactors of *CcO* shown in Figure 1. The pK_a's are compared for the different dielectric constants of water-filled cavities (ϵ = 15, 20, or 80). In all calculations, the dielectric constants of the QM system and protein part are set to 1 and 4, respectively.

inner water molecules most likely is related to a higher value of the dielectric constant.

Our general conclusion is that the pumping scheme of *CcO* proposed in this and in the previous papers is valid in surprisingly wide range of possible values of the dielectric for the cavities; namely, for values greater than roughly 10, the general pumping scheme emerging from this work remains the same. This is an encouraging result, because the exact value of this parameter would be difficult to control by the enzyme.

IV. Conclusions

We have calculated the pK_a values of His291 and Glu242, the two key residues of the proposed proton pumping mechanism in bovine *CcO*. The active site Cu_B complex was treated by density functional theory, while the effects of the protein charges and solvation were incorporated using the continuum electrostatic calculations.

Our model does not account for any protein dynamic effects and deals only with a fixed crystal structure. The dielectric constants are chosen in an empirical way, as usual in such calculations, and therefore the obtained results should be considered keeping the limitations of the model in mind. The choice of the dielectric constants for a protein and the protein cavities that may contain internal water has been a topic of active debate for a very long time (see refs 68 and 90−94, a discussion of a new procedure with optimized dielectric constants,[95] and references therein). We choose the dielectric constants in the same way as it was done in a recent similar DFT/electrostatic studies.[23,25,28,29] The good agreement between calculated and measured pK_a of the Glu242 residue, for instance, gives us also reason to believe that although not perfect our model still manages to account for most of the electronic and electrostatic energies of this complex system in a reasonably accurate way.

The pK_a values were calculated for several redox states of the enzyme, and the influence of different factors on the pK_a values was analyzed in detail. We were particularly interested in determining factors that would make it possible for this complex system to work as a proton pump. To accomplish this goal, we considered several computational models and results of these calculations are briefly summarized here.

In the aqueous phase, the pK_a of Glu242 is 4.4; the His291 ligand of the oxidized Cu_B center has a pK_a of 8.6, and in the reduced form the pK_a is 13.2. Therefore, the aqueous phase acidities need to be significantly shifted by the protein environment in order for this pair to work as a pump element.

Interestingly, already by solvating the Cu_B center in a continuum low dielectric environment, model b, the redox-dependence of the His291 pK_a value is achieved. Here, the corresponding pK_a's are −9.9 and +9.8 for the oxidized and reduced complex, respectively. However, at the same time the pK_a of Glu242 is 14.5, which means that for the reduced state of the Cu_B center, a proton cannot be pulled up from Glu to His site. Under these conditions this process is energetically unfavorable.

The dielectric inhomogeneities and water-filled cavities, model d, increase the pK_a's of His291 in both redox states (−3.7 and +10.4) and slightly decrease the pK_a of Glu242 to 12.0. However, the qualitative conclusions here are the same: there is a redox-dependent acidity of the His291 site, but still Glu possesses a pK_a 2 units higher than His, and a hypothetical transfer of a pump proton from Glu242 to His291 would be energetically unfavorable.

Inclusion of the protein charges, which are found in a self-consistent manner, model e, finely tunes the pK_a values to become suitable for proton pumping. Namely, the pK_a's of His291 increase further by 6−9 pK_a units, and at the same time, the pK_a of Glu242 slightly decreases or remains the same depending on the redox state of the heme *a*, see Figure 5. Table 7 compares the pK_a's of these two residues for the different redox states of the enzyme. We find that for a given redox state of the binuclear complex, additional electrons on two other redox centers (Cu_A and heme *a*) only slightly modify the Glu242 and His291 pK_a values.

Based on the calculated pK_a values, the proton transfer from Glu242 to His291 can only occur after electron transfer to the binuclear center of the enzyme. For example, the reduction of the heme *a* increases the pK_a of Glu242 by about 2 units, making it more difficult to transfer a proton to His291 before an electron is transferred further to the catalytic center of the enzyme.

Comparing the effects of the addition of the protein charges to continuum and inhomogeneous dielectric environments, we concluded that the internal protein cavities, presumably filled with water, appear to play a very important role and have a huge influence on the pK_a values of the buried residues, with which they are in (direct) contact. The reason, obviously, is the high dielectric constant associated with the cavities and their screening effect.

The effects of different factors on the pK_a values are summarized in Figure 5. As shown in this figure, going from the aqueous phase to a low dielectric continuum, the pK_a's change by −18.8, −3.4, and +10.1, for His-oxidized Cu_B, His-reduced Cu_B, and Glu site, respectively. Introducing dielectric inhomogeneities, the Born solvation energy changes so as to shift the pK_a by +6.2, +0.6, and −2.5 units, respectively. Addition of the protein charges causes shifts of +5.8, +7.0, and −2.5 pK_a units, respectively. Finally, the screening effects of the protein inner water cavities and external high dielectric solvent are estimated to be −13.0, −19.0, and −14.5 units, respectively.

It has been shown that the pK_a of His 291 depends very strongly on the redox state of the Cu_B center, while a much weaker dependence is observed for Glu242, and its pK_a values remain relatively high for all redox states of the enzyme (see Table 7). This is not surprising, given that His291 is located much closer to a redox center than Glu242. Also, since in the reduced state of Cu_B His291 is protonated while in the oxidized state His291 is deprotonated, the total charge of Cu_B *together* with its ligand His291 does not change, and hence the redox state of the Cu_B center has much less effect on the pK_a of a

distant Glu242 residue. We find rather that the pK_a of Glu242 is coupled to the redox state of the adjacent heme *a*. This dependence is less than 3 pK_a units, yet can be important. Each time Glu242 donates a proton, it needs to get reprotonated; hence the obtained high pK_a values of Glu242 totally make sense.

Overall, the obtained results support our earlier proposal[2] that the His291 ligand of the Cu_B center works as a proton pump element in *CcO*, and Glu242 is a proton donor for both pumped and chemical protons.

Acknowledgment. We thank Xuehe Zheng for his helpful input. This work has been supported by the NSF grant and a research grant from the NIH (GM54052).

Supporting Information Available: Solvation free energies of the Cu_B complex in different redox states of the protein and solvation free energies of glutamic acid in aqueous phase, uniform low dielectric medium ($\epsilon = 4$), and inhomogeneous protein environment. This material is available free of charge via the Internet at http://pubs.acs.org.

Abbreviations

CcO, cytochrome *c* oxidase
MeIm, methylimidazole
QM, quantuum mechanical
PBE, Poisson−Boltzmann equation
PE, Poisson equation
SCRF, self-consistent reaction field
The numbering refers to bovine *CcO*.

References and Notes

(1) Popovic, D. M.; Stuchebrukhov, A. A. *J. Am. Chem. Soc.* **2004**, *126*, 1858.
(2) Popovic, D. M.; Stuchebrukhov, A. A. *FEBS Lett.* **2004**, *566*, 126.
(3) Wikström, M. *Curr. Opin. Struct. Biol.* **1998**, *8*, 480.
(4) Gennis, R. B. *Proc. Natl. Acad. Sci. U.S.A.* **1998**, *95*, 12747.
(5) Michel, H.; Behr, J.; Harrenga, A.; Kannt, A. *Annu. Rev. Biophys. Biomol. Struct.* **1998**, *27*, 329.
(6) Babcock, G. T.; Wikström, M. *Nature* **1992**, *356*, 301.
(7) Ferguson-Miller, S.; Babcock, G. T. *Chem. Rev.* **1996**, *7*, 2889.
(8) Wikström, M.; Jasaitis, A.; Backgren, C.; Puustinen, A.; Verkhovsky, M. I. *Biochim. Biophys. Acta* **2000**, *1459*, 514.
(9) Zaslavsky, D.; Gennis, R. B. *Biochim. Biophys. Acta* **2000**, *1458*, 164.
(10) Michel, H. *Biochemistry* **1999**, *38*, 15129.
(11) Wikström, M. *Biochemistry* **2000**, *39*, 3515.
(12) Han, S.; Takahashi, S.; Rousseau, D. L. *J. Biol. Chem.* **2000**, *275*, 1910.
(13) Yoshikawa, S.; Shinzawa-Itoh, K.; Nakashima, R.; Yaono, R.; Yamashita, E.; Inoue, N.; Yao, M.; Fei, M. J.; Libeu, C. P.; Mizushima, T.; Yamaguchi, H.; Tomizaki, T.; Tsukihara, T. *Science* **1998**, *280*, 1723.
(14) Stuchebrukhov, A. A. *J. Theor. Comput. Chem.* **2003**, *2*, 91.
(15) Rich, P. R. *Aust. J. Plant Physiol.* **1995**, *22*, 479.
(16) Ädelroth, P.; Svensson-Ek, M.; Mitchell, D. M.; Gennis, R. B.; Brzezinski, P. *Biochemistry* **1997**, *36*, 13824.
(17) Verkhovskaya, M. L.; Garcia-Horsman, A.; Puustinen, A.; Rigaud, J.-L.; Morgan, J. E.; Verkhovsky, M. I.; Wikström, M. *Proc. Natl. Acad. Sci. U.S.A.* **1997**, *94*, 10128.
(18) Iwaki, M.; Rich, P. R. *J. Am. Chem. Soc.* **2004**, *126*, 2386.
(19) Wikström, M. *Biochim. Biophys. Acta* **2000**, *1458*, 188.
(20) Chen, J. L.; Noodleman, L.; Case, D. A.; Bashford, D. *J. Phys. Chem.* **1994**, *98*, 11059.
(21) Li, J.; Fischer, C. L.; Chen, J. L.; Bashford, D.; Noodleman, L. *J. Phys. Chem.* **1996**, *96*, 2855.
(22) Kallies, B.; Mitzner, R. *J. Phys. Chem. B* **1997**, *101*, 2959.
(23) Richardson, W. H.; Peng, C.; Bashford, D.; Noodleman, L.; Case, D. A. *Int. J. Quantum Chem.* **1997**, *61*, 207.
(24) Topol, I. A.; Tawa, G. J.; Burt, S. K.; Rashin, A. A. *J. Phys. Chem. A* **1997**, *101*, 10075.
(25) Ullmann, G. M.; Noodleman, L.; Case, D. A. *J. Biol. Inorg. Chem.* **2002**, *7*, 632.
(26) Quenneville, J.; Popovic, D. M.; Stuchebrukhov, A. A. *J. Phys. Chem. B* **2004**, *108*, 18383.
(27) Mouesca, J. M.; Chen, J. L.; Noodleman, L.; Bashford, D.; Case, D. A. *J. Am. Chem. Soc.* **1994**, *116*, 11898.
(28) Li, J.; Nelson, M. R.; Peng, C. Y.; Bashford, D.; Noodleman, L. *J. Phys. Chem. A* **1998**, *102*, 6311.
(29) Li, J.; Fisher, C. L.; Konecny, R.; Bashford, D.; Noodleman, L. *Inorg. Chem.* **1999**, *38*, 929.
(30) Warshel, A. *Biochemistry* **1981**, *20*, 3167.
(31) Warshel, A. *Acc. Chem. Res.* **1981**, *14*, 284.
(32) Bashford, D.; Gerwert, K. *J. Mol. Biol.* **1992**, *224*, 473.
(33) Bashford, D. An object-oriented programming suite for electrostatic effects in biological molecules. In *Scientific Computing in Object-Oriented Parallel Environments*; Ishikawa, Y., Oldehoeft, R. R., Reynders, J. V. W., Tholburn, M., Eds.; Springer: Berlin, 1997; Vol. 1343, p 233.
(34) Hohenberg, P.; Kohn, W. *Phys. Rev.* **1964**, *136*, B864.
(35) Kohn, K.; Sham, L. J. *Phys. Rev.* **1965**, *140*, A1133.
(36) *Jaguar 5.5*, S., L. L. C., Portland, OR, 1991−2003 ed.
(37) Becke, A. D. *J. Chem. Phys.* **1993**, *98*, 5648.
(38) Hay, P. J.; Wadt, W. R. *J. Chem. Phys.* **1985**, *82*, 299.
(39) Ditchfield, R.; Hehre, W. J.; Pople, J. A. *J. Chem. Phys.* **1971**, *54*, 724.
(40) Hehre, W. J.; Pople, J. A. *J. Chem. Phys.* **1972**, *56*, 4233.
(41) Hehre, W. J.; Ditchfield, R.; Pople, J. A. *J. Chem. Phys.* **1972**, *56*, 2257.
(42) Binkley, J. S.; Pople, J. A. *J. Chem. Phys.* **1977**, *66*, 879.
(43) Hariharan, P. C.; Pople, J. A. *Theor. Chim. Acta* **1973**, *28*, 213.
(44) Francl, M. M.; Pietro, W. J.; Hehre, W. J.; Binkley, J. S.; Gordon, M. S.; DeFrees, D. J.; Pople, J. A. *J. Chem. Phys.* **1982**, *77*, 3654.
(45) Clark, T.; Chandrasekhar, J.; Spitznagel, G. W.; Schleyer, P. v. R. *J. Comput. Chem.* **1983**, *4*, 294.
(46) Frisch, M. J.; Pople, J. A.; Binkley, J. S. *J. Chem. Phys.* **1984**, *80*, 3265.
(47) Krishnan, R.; Binkley, J. S.; Seeger, R.; Pople, J. A. *J. Chem. Phys.* **1980**, *72*, 650.
(48) McLean, A. D.; Chandler, S. G. *J. Chem. Phys.* **1980**, *72*, 5639.
(49) Blomberg, M. R. A.; Siegbahn, P. E. M.; Babcock, G. T.; Wikström, M. *J. Am. Chem. Soc.* **2000**, *122*, 12848.
(50) Siegbahn, P. E. M.; Blomberg, M. R. A.; Blomberg, M. L. *J. Phys. Chem. B* **2003**, *107*, 10946.
(51) Tannor, D. J.; Marten, B.; Marphy, R.; Friesner, R. A.; Sitkoff, D.; Nicholls, A.; Ringnalda, M. G. W. A. I.; Honig, B. *J. Am. Chem. Soc.* **1994**, *116*, 11875.
(52) Marten, B.; Kim, K.; Cortis, C.; Friesner, R. A.; Murphy, R. B.; Ringnalda, M. N.; Sitkoff, D.; Honig, B. *J. Phys. Chem.* **1996**, *100*, 11775.
(53) Breneman, C. M.; Wiberg, K. B. *J. Comput. Chem.* **1990**, *11*, 361.
(54) Bashford, D.; Karplus, M. *Biochemistry* **1990**, *29*, 10219.
(55) Nicholls, A.; Honig, B. *J. Comput. Chem.* **1991**, *12*, 435.
(56) Bashford, D.; Karplus, M. *J. Phys. Chem.* **1991**, *95*, 9557.
(57) Beroza, P.; Fredkin, D. R.; Okamura, M. Y.; Feher, G. *Proc. Natl. Acad. Sci. U.S.A.* **1991**, *88*, 5804.
(58) Gunner, M. R.; Honig, B. *Proc. Natl. Acad. Sci. U.S.A.* **1991**, *88*, 9151.
(59) Yang, A.-S.; Gunner, M. R.; Sompogna, R.; Honig, B. *Proteins: Struct. Funct. Genet.* **1993**, *15*, 252.
(60) Beroza, P.; Case, D. A. *J. Phys. Chem.* **1996**, *100*, 20156.
(61) Baptista, A. M.; Martel, P. J.; Soares, C. M. *Biophys. J.* **1999**, *76*, 2978.
(62) Popovic, D. M.; Zaric, S. D.; Rabenstein, B.; Knapp, E. W. *J. Am. Chem. Soc.* **2001**, *123*, 6040.
(63) Popovic, D. M.; Zmiric, A.; Zaric, S. D.; Knapp, E. W. *J. Am. Chem. Soc.* **2002**, *124*, 3775.
(64) Rabenstein, B. Karlsberg online manual. http://lie.chemie.fu-berlin/karlsberg/ ed., 1999.
(65) Sharp, K.; Honig, B. *Annu. Rev. Biophys. Biophys. Chem.* **1990**, *19*, 301.
(66) Simonson, T.; Perahia, D. *Proc. Natl. Acad. Sci. U.S.A.* **1995**, *92*, 1082.
(67) Simonson, T.; Brooks, C. L. *J. Am. Chem. Soc.* **1996**, *118*, 8452.
(68) Warshel, A.; Papazyan, A. *Curr. Opin. Struct. Biol.* **1998**, *8*, 211.
(69) MacKerell, J. A. D.; Bashford, D.; Bellot, M.; Dunbrack, J. R. L.; Evanseck, J. D.; Field, M. J.; Fischer, S.; Gao, J.; Guo, H.; Ha, S.; Joseph-McCarthy, D.; Kuchnir, L.; Kuczera, K.; Lau, F. T. K.; Mattos, C.; Michnick, S.; Ngo, T.; Nguyen, D. T.; Prodholm, B.; Reiher, I. W. E.; Roux, B.; Schlenkrich, M.; Smith, J. C.; Stote, R.; Straub, J.; Watanabe, M.; Wiórkiewicz-Kuczera, J.; Yin, D.; Karplus, M. *J. Phys. Chem.* **1998**, *102*, 3586.
(70) Tanokura, M. *Biochim. Biophys. Acta* **1983**, *742*, 576.
(71) Tanford, C. *Adv. Protein Chem.* **1962**, *17*, 69.
(72) Tanford, C.; Roxby, R. *Biochemistry* **1972**, *11*, 2192.
(73) Nozaki, Y.; Tanford, C. *J. Biol. Chem.* **1967**, *242*, 4731.
(74) Lübben, M.; Gerwert, K. *FEBS Lett.* **1996**, *397*, 303.
(75) Hellwig, P.; Rost, B.; Kaiser, U.; Ostermeier, C.; Michel, H.; Mantele, W. *FEBS Lett.* **1996**, *385*, 53.

(76) Puustinen, A.; Bailey, J. A.; Dyer, R. B.; Mecklenberg, S. L.; Wikström, M. *Biochemistry* **1997**, *36*, 13195.
(77) Hellwig, P.; Behr, J.; Ostermeier, C.; Richter, O.-M. H.; Pfitzner, U.; Odenwald, A.; Ludwig, B.; Michel, H.; Mantele, W. *Biochemistry* **1998**, *37*, 7390.
(78) Lübben, M.; Prutsch, A.; Mamat, B.; Gerwert, K. *Biochemistry* **1999**, *38*, 2048.
(79) Namslauer, A.; Aagaard, A.; Katsonouri, A.; Brzezinski, P. *Biochemistry* **2003**, *42*, 1488−1498.
(80) Ostermeier, C.; Harrenga, A.; Ermler, U.; Michel, H. *Proc. Natl. Acad. Sci. U.S.A.* **1997**, *94*, 10547.
(81) Svensson-Ek, M.; Abramson, J.; Larsson, G.; Tornroth, S.; Brzezinski, P.; Iwata, S. *J. Mol. Biol.* **2002**, *321*, 329.
(82) Tsukihara, T.; Shimokata, K.; Katayama, Y.; Shimada, H.; Muramoto, K.; Aoyama, H.; Mochizuki, M.; Shinzawa-Itoh, K.; Yamashita, E.; Yao, M.; Ishimura, Y.; Yoshikawa, S. *Proc. Natl. Acad. Sci. U.S.A.* **2003**, *100*, 15304.
(83) Tsukihara, T.; Aoyama, H.; Yamashita, E.; Tomizaki, T.; Yamaguchi, H.; Shinzawa-Itoh, K.; Nakashima, R.; Yaono, R.; Yoshikawa, S. *Science* **1996**, *272*, 1136.
(84) Garcia, A. E.; Hummer, G. *Proteins* **2000**, *38*, 261−272.
(85) Backgren, C.; Hummer, G.; Wikström, M.; Puustinen, A. *Biochemistry* **2000**, *39*, 7863−7867.
(86) Schmidt, B.; McCracken, J.; Ferguson-Miller, S. *Proc. Natl. Acad. Sci. U.S.A.* **2003**, *100*, 15539−15542.
(87) Zheng, X.; Medvedev, D. M.; Swanson, J.; Stuchebrukhov, A. A. *Biochim. Biophys. Acta* **2003**, *1557*, 99.
(88) Wikström, M.; Verkhovsky, M. I.; Hummer, G. *Biochim. Biophys. Acta* **2003**, *1604*, 61.
(89) Olkhova, E.; Hutter, M. C.; Lill, M. A.; Helms, V.; Michel, H. *Biophys. J.* **2004**, *86*, 1873−1889.
(90) Warshel, A.; Russel, S. T. *Q. Rev. Biophys.* **1984**, *17*, 283.
(91) Gilson, M. K.; Honig, B. *Biopolymers* **1986**, *25*, 2097.
(92) Harvey, S. C. *Proteins* **1989**, *5*, 78.
(93) Warshel, A.; Aqvist, J. *Annu. Rev. Biophys. Biophys. Chem.* **1991**, *20*, 267.
(94) Gilson, M. K. *Curr. Opin. Struct. Biol.* **1995**, *5*, 216.
(95) Wojciechowski, M.; Grycuk, T.; Antosiewicz, J. M.; Lesyng, B. *Biophys. J.* **2003**, *84*, 750.